Academic Journal of Science and Technology
ISSN: 2771-3032 | Vol. 5, No. 3, 2023

Sandstone Impact Damage Study

Xiaohui Guo[1, *]

[1] School of Civil Engineering, Henan Polytechnic University, Jiaozuo 454000, China
[*] **Corresponding author**: 2578196020@qq.com

Abstract: In order to study the impact of impact on sandstone, dynamic impact is conducted on sandstone through drop hammer test, wave velocity test is conducted on the impacted specimen by using wave velocity instrument, and the damage effect of impact on sandstone is analyzed by using wave velocity damage calculation formula. The results show that the greater the impact velocity, the smaller the measured wave velocity and the greater the damage to the sandstone.

Keywords: Lash, Drop weight test, Wave velocity, Harm.

1. Introduction

At present, energy plays a key role in China's economic development, however, more than 90% of coal seams in China are low permeability, in order to improve the utilization rate of coalbed methane, a variety of methods have been researched at home and abroad, such as hydraulic fracturing[1-3], hydraulic slitting[4-6], Mechanical cavity making[7] and gas phase fracturing[8-9] technologies, but the effect of increasing permeability of coal seams by using water power to increase permeability has limitations, the number of fractures is too small and the effect of increasing permeability is not obvious, while The cost of gas-phase fracturing is high, therefore, studying the effect of impact action on coal seam permeability increase is one of the current priorities. Zhang Dongming and Bai Xin et al [10-11] established a liquid CO_2 phase change gas jet pressure model, and theoretically analyzed the mechanical mechanism of liquid CO_2 phase change shot hole breaking and the mechanical mechanism of fracture extension under ground stress conditions based on theories of thermal engineering, elasticity mechanics, and fracture mechanics, and determined the dominant fracturing direction of liquid CO_2 phase change directional shot hole in the test area, which effectively increased the porosity of coal samples, the The pore size, specific surface area, and visible pore ratio of coal samples were effectively increased, which improved the pore structure and percolation capacity in the coal body. Hu Shisheng et al [12] conducted a systematic study on the damage softening effect of concrete materials after impact loading by using the "damage freezing" method based on the impact compression test with Hopkinson compression bars, and gave the damage evolution equation of concrete under impact loading, and combined with the viscoelastic principal structure theory to summarize the damage linear viscoelastic principal structure of concrete materials. Basnthia [13] showed by two different impact load tests on a falling hammer testing machine that the energy absorbed into the concrete specimen under impact loading is more than that of static loading. Wu Mingxin et al [14-15] investigated the drop hammer test on concrete and combined the numerical simulation of the fine view model to investigate the dynamic impact performance and damage mechanism of concrete, which proved the validity and reasonableness of the fine view model.Zhang [16] et al. used different loading rates and performed drop hammer tests on the specimens and found that the lower loading rates had a more significant effect on the crack initiation rate, and the crack initiation rate at high loading Lin Lang [17] et al. studied large-size specimens with arc-bottom trapezoidal opening structure and calculated the crack length and crack velocity using fractal method.

In conclusion, the study of coal seam damage by impact loading is necessary and can provide theoretical support for the study of the damage mechanism of coal seams.

2. Drop Hammer Impact Test

2.1. Testing device

The device used in this experiment consists of two parts, one is a white PVC pipe with multiple 3 cm × 10 cm openings in the middle to reduce air resistance, and in its lower part, a green PVC pipe is set to fix the sandstone, as shown in Figure 1.

(a) Falling hammer impact device (b) Partial view of the installation

Figure 1. Dropevette Stedevis

2.2. Test procedure

(1) Sandstone surface is polished smooth and wrapped with cling film for one week.

(2) Putting the finishing sandstone inside the green PVC pipe with shims on the lower part.

(3) A thin wire is tied to the upper part of the drop hammer, and the drop hammer is made to impact test the sandstone at different speeds by adjusting the drop height.

(4) After the impact of the drop hammer, the sandstone is measured by wave velocity meter and the data is recorded for the next test.

2.3. Test results

The sandstone received different degrees of damage and destruction during the impact of the falling hammer. At a drop height of 1.5 m, the sandstone as a whole did not show large changes; at a drop height of 2 m, the upper surface of the sandstone began to show debris; at a drop height of 2.5 m, debris fell off from the upper part of the sandstone, and small cracks of about 0.5 cm in length began to appear in the upper part. Under the impact of the falling hammer at a height of 3m, the cracks on the surface of the sandstone had a tendency to extend downward, and more pieces fell off from the upper part of the sandstone, and under the impact of the falling hammer at a height of 3.5m, large pieces fell off from the sandstone, the cracks extended downward, and the upper part of the sandstone had a tendency to be smashed, and under the impact of the falling hammer at a height of 4m, a macroscopic fracture surface appeared, and the sandstone was completely impacted into pieces and slag. The specimen after the impact is shown in Figure 2.

Figure 2. Drawing of the test piece after impact

During the process before and after conducting the drop hammer test, the wave velocity of the sandstone was measured with a wave velocity meter for each impact and the data was recorded as shown in Table 1.

Table 1. Change of wave velocity before and after impact

Drop height (m)	Initial wave speed (km/s)	Wave speed after the first impact (km/s)	Wave speed after the second impact (km/s)	Wave speed after the third impact (km/s)	Wave speed after the fourth Impact (km/s)
1.5	2.813	2.306	2.134	1.708	/
2	2.051	1.706	1.348	0.955	/
2.5	2.827	2.544	2.100	1.980	/
3	2.553	1.814	1.413	0.584	/
3.5	2.212	1.732	1.234	0.967	/
4	2.019	1.226	1.054	1.022	/

Changes in internal micro-pores and micro-cracks in sandstone before and after impact will cause changes in the ultrasonic waves released by the wave velocity meter, so that changes in internal crack damage in sandstone can be expressed by wave velocity as follows.

$$D_n = 1 - \left(\frac{V_n}{V_0} \right)^2 \tag{1}$$

where V_n is the measured wave velocity of the specimen after each load impact, and V_0 is the measured wave velocity of the specimen in the initial state.

According to Equation 2-1, we can get Table 2.

Table 2. Impact damage

Drop height (m)	Damage D2	Damage D2	Damage D3	Damage D4
1.5	0.329	0.427	0.634	1.000
2	0.309	0.573	0.788	1.000
2.5	0.175	0.443	0.511	1.000
3	0.510	0.712	0.893	1.000
3.5	0.397	0.701	0.818	1.000
4	0.640	0.736	0.753	1.000

3. Numerical Simulation of Impact Damage

According to the damage effects of sandstone under the action of falling hammer impact, ANSYS software was used to simulate and study the dynamic damage of sandstone microstructure, visualize the damage of sandstone, and explore the microscopic damage mechanism of sandstone.

3.1. Damage to the intrinsic structure relationship

The damage process of sandstone can be divided into three stages, which are linear elastic stage, elasto-plastic stage and plastic softening stage, representing I - no damage, II - micro-crack evolution, III - macro-crack nucleation stage in the process of fracture damage evolution inside the specimen, the geometric model curve of damage evolution is shown in

Figure 3, where OA_1 is the elastic stage, in this stage, there is no obvious damage to the material, A_1A is the elastic-plastic stage, in this stage, there will be micro-cracks generated, the specimen surface cracks are not obvious, AB is the macro-crack nucleation stage, in this stage, the specimen generated by the cracks began to randomly connect, forming macro-cracks, and finally nucleation, BC is the crack expansion stage, in this stage, the macro-crack nucleus occurs rapid expansion until through the entire material unit. Where point B is the material fracture brittle-tough transformation point, before point B, the material fracture shows brittle development, after point B, the material fracture starts to transform from brittle expansion to tough expansion.

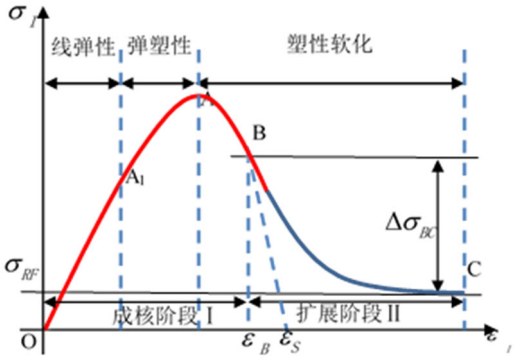

Figure 3. Basic mode of damage evolution

The expression for the main compressive stress damage evolution of the material is

$$D=\begin{cases}\left(\dfrac{\varepsilon_I}{\varepsilon_s}\right)^{\mathrm{m}}, 0<\varepsilon_I\le\varepsilon_B \\ 1-\left(\dfrac{\left(\Delta\sigma_{BC}\right)^2}{\left(\varepsilon_B-\varepsilon_I\right)k_B+\Delta\sigma_{BC}}+\sigma_{RF}\right)\dfrac{1}{E_0\varepsilon_I}, \varepsilon_B<\varepsilon_I\end{cases} \tag{2}$$

Among them, D is the damage variable, ε_I is the principal compressive strain, ε_S is the brittle fracture endpoint value, m is the brittle index, and the intersection point of the tangent line at point B and the transverse axis is ε_S . ε_B represents the transformation strain from microcrack evolution to macroscopic fracture, E_0 is the initial elastic modulus of the material, σ_{RF} is residual stress, k_B is the stress reduction rate corresponding to point B, and $\Delta\sigma_{BC}$ is the residual stress. The calculation formula is as follows:

$$\Delta\sigma_{BC}=E_0\left[1-\left(\frac{\varepsilon_B}{\varepsilon_I}\right)^m\right]\varepsilon_B-\sigma_{RF} \tag{3}$$

$$k_B=\left[1-\left(\frac{\varepsilon_b}{\varepsilon_S}\right)^m(m+1)\right]E_0 \tag{4}$$

According to the elastic damage relationship equation $E=E_0\left(1-D\right)$, the uniaxial principal compressive stress - principal compressive strain equation is

$$\sigma_I=\begin{cases}E_0\left[1-\left(\dfrac{\varepsilon_I}{\varepsilon_S}\right)^m\right]\varepsilon_I, & \varepsilon_I<\varepsilon_B \\ \dfrac{\left(\Delta\sigma_{BC}\right)^2}{\left(\varepsilon_I-\varepsilon_B\right)k_B+\Delta\sigma_{BC}}+\sigma_{RF}, \varepsilon_I\ge\varepsilon_B\end{cases} \tag{5}$$

3.2. Numerical simulation results

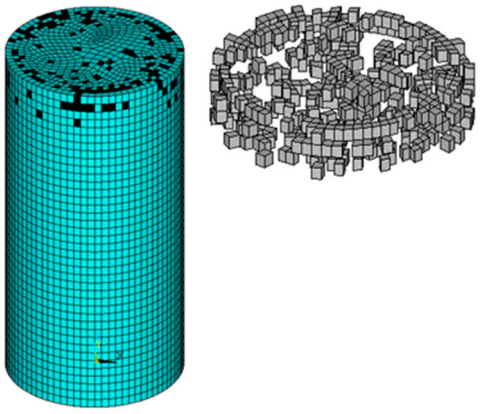

Model picture Damage spot map

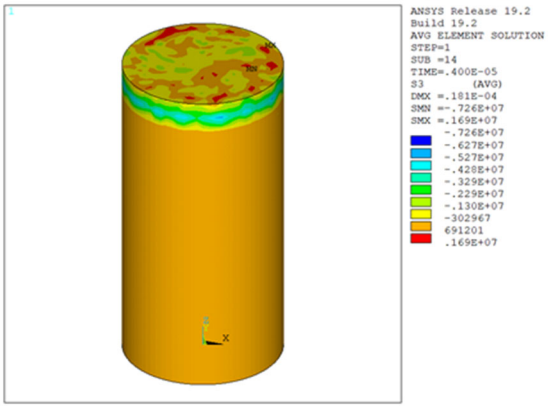

Stress cloud map

(a) t=0.05ms

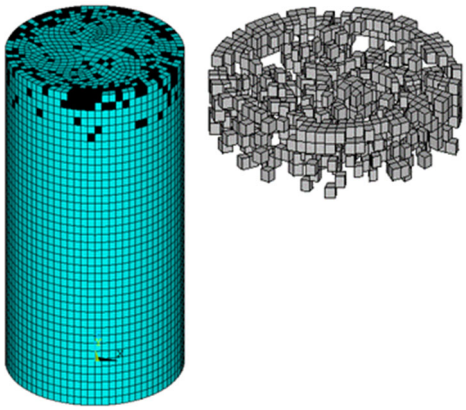

Model picture Damage spot map

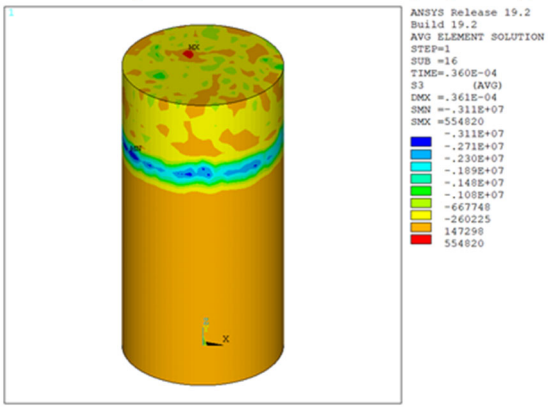

Stress cloud map
(b) t=0.10ms

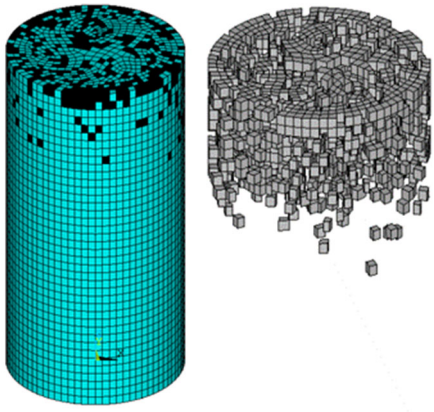

Model picture Damage spot map

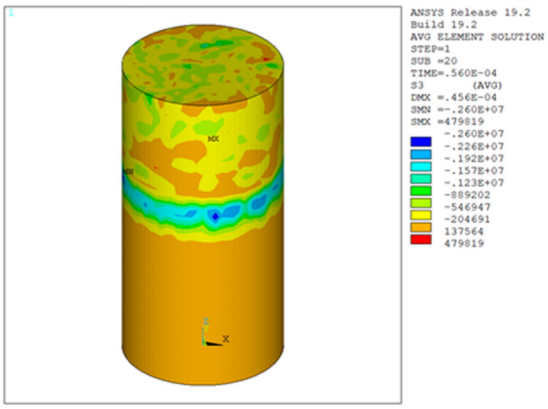

Stress cloud map
(d) t=0.20ms

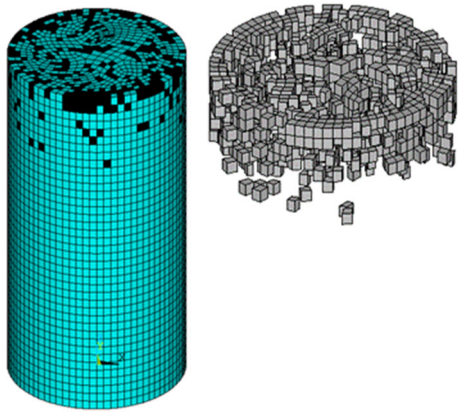

Model picture Damage spot map

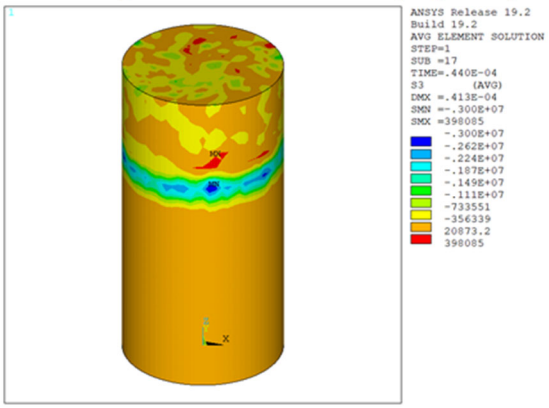

Stress cloud map
(c) t=0.15ms

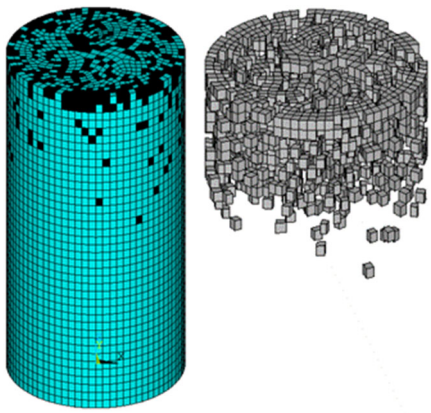

Model picture Damage spot map

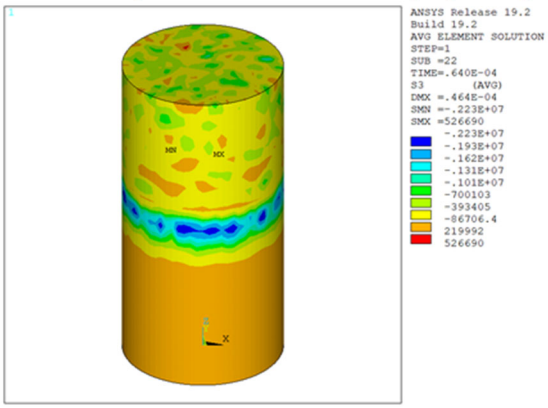

Stress cloud map
(e) t=0.25ms

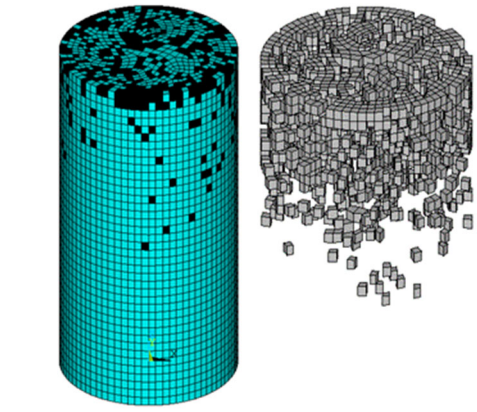

Model picture Damage spot map

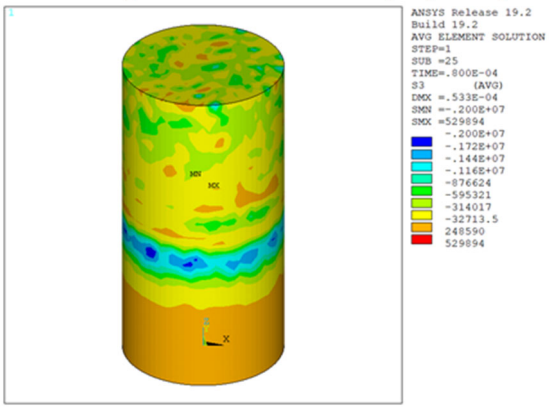

Stress cloud map

(f) t=0.30ms

Figure 4. Model damage evolution diagram

Figure 4 shows the damage evolution diagram of numerical simulation, where the black part of the model diagram is the damage unit, and all the damage units are put forward to form the damage spot diagram, and the stress cloud diagram of the sandstone can be seen to change during the impact process. With the increase of impact velocity, the number of damage units of sandstone is also increasing, and they are connected with each other, forming fissures inside, and continue to extend and expand downward, causing the damage of sandstone to gradually increase; during the impact process, the stress suffered by the sandstone is also transferred downward from the upper surface, causing some impact on the sandstone as a whole.

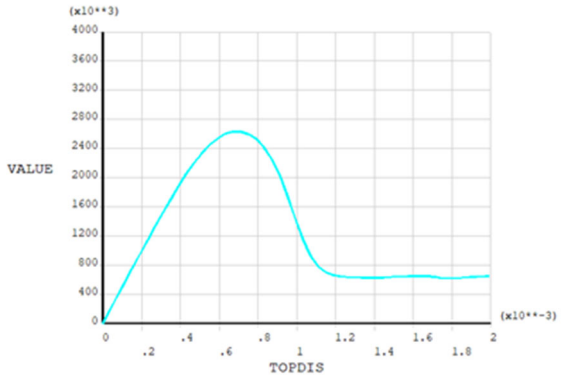

Figure 5. Bearing capacity curve

Figure 5 shows the bearing capacity curves of the four ratios under the action of cyclic impact, and it can be seen from the figure that the specimens all went through four stages during the impact: compression-density stage, linear elastic deformation stage, microcrack expansion stage and damage stage. It can be seen from the figure that when the stress reaches the peak and continues to load, the specimen begins to show damage, and the curve shows a linear downward trend, at which time the specimen is brittle damage, in line with the damage characteristics of brittle materials.

4. Conclusion

a.During the impact, the greater the impact velocity, the more damage units in the sandstone, and the greater the damage caused.

b. Under the action of multiple impact loads, cracks appear inside the sandstone and damage is formed, which makes the measured wave velocity decrease.

c. The damage process of sandstone goes through four stages: compression-density stage, linear elastic deformation stage, microcrack expansion stage and damage stage.

References

[1] X. C.,Li, Permeability enhancement pathway to improve the extraction effect of single low permeability coal seam[J] Coal mine safety, 2011,42(04):90-92.

[2] B. X. Xun Hydraulic Pressurized Cracking and Permeability Improvement Technology Applied to Gas Drainage. [J]Coal Carbon Technology Science,2010,38(11):78-80+119.

[3] C. J. Xu, Experimental Study on Hydraulic Fracturing Permeability Improvement Technology in High Gas and Low Permeability Coal Seam.[J] Coal Technology,2014,33(05):28-30.

[4] X. E. Chen, Application of Hydraulic Slot Cutting Technology to ImproveGas Drainage Effect [J] Coal Engineering, 2011, No.394(08):34-36.

[5] E. Y. Song, Principle of Gas Extraction by Increasing Permeability ofCoal Seam with Hydraulic Cutting and Its Application.[J] Chinese Journal of Safety Science 2011, 21(04):78-82.

[6] X. Y. Zhang, The Mechanism Research of Preventing Heading Face Gas Outburst by Hydraulic Cutting Seam.[D] Taiyuan University of Technology,2012.

[7] Q. B. Mou, Study on enhanced gas drainage technology of borehole gasbased on mechanical borehole reaming.[J] Coal Science and Technology, 2015,43(05):58-61+86.

[8] F. L. Li. Technology of high-speed driving and outburst elimination by CO2 gas fracturing in Yuxi coal mine.[J] China Mining Industry, 2020,29(04):146-151.

[9] Z. F. Wang, Experiment research on strengthening gas drainage effect with fracturing technique by liquid CO2 phase transition.[J] Henan University of Technology Newspaper (Natural Science Edition), 2015,34(01):1-5.

[10] X. Bai, Pressure variation and coal fracturing law of liquid CO2 phase transition jet.[J] Journal of China University of Mining and Technology, 2020,49(04):661-670.

[11] D. M. Zhang, Research and application on technology of increased permeability by liquid CO2 phase change directional jet fracturing in low-permeability coal seam.[J] Journal of Coal Industry, 2018,43(07):1938-1950.

[12] Y. Wang, Study of the dynamic fracture characteristics of coal with a bedding structure based on the NSCB impact test. Engineering Fracture Mechanics, 184, 319–338.

[13] Banthia N, Mindess S, Bentur A, et al. Impact testing of concrete using a drop-weight impact machine [J].Experimental Mechanics, 1989, 29(l):63-69.

[14] Wu, M.,Study on Dynamic Impact Behavior of Concrete through Experimental Tests and Meso-scale Simulation.[D] Tsinghua University,2015.

[15] Wu, M., Zhang, C., & Chen, Z. (2016). Drop-weight tests of concrete beams prestressed with unbonded tendons and meso-scale simulation. International Journal of Impact Engineering, 93, 166–183.

[16] X. X. Zhang, Effect of loading rate on crack velocities in HSC. International Journal of Impact Engineering, 37(4), 359–370.

[17] L. Lang, Study of crack arrest mechanism and dynamic behaviour using arc-bottom specimen under impacts. Fatigue & Fracture of Engineering Materials & Structures.